JGR Space Physics

RESEARCH ARTICLE
10.1029/2021JA029458

Key Points:

- Peak proton fluxes with energies >20 MeV at $L = 6.6$ on $10th$ September were >2 order higher than the ones observed on September 7, 2017
- Solar proton fluxes were observed as close as L~3.4
- Solar proton fluxes show no particular magnetic local time dependence

Correspondence to:
B. Veenadhari,
veenadhari.b@iigm.res.in

Citation:
Pandya, M., & Bhaskara, V. (2021). Quantitative assessment of protons during the solar proton events of September 2017. *Journal of Geophysical Research: Space Physics*, *126*, e2021JA029458. https://doi.org/10.1029/2021JA029458

Received 17 APR 2021
Accepted 9 SEP 2021

Quantitative Assessment of Protons During the Solar Proton Events of September 2017

Megha Pandya[1] and Veenadhari Bhaskara[1]

[1]Indian Institute of Geomagnetism, Navi Mumbai, India

Abstract We present multi-spacecraft observations of the proton fluxes spanning from 1.5 to 433 MeV for the largest solar proton event of solar cycle 24, i.e., September 7 and 10, 2017. In September 2017, M5.5 flare on September 4, X9.3 flare on September 6 and X8.2 flare on September 10 gave rise to solar proton event when observed by near-Earth spacecrafts. On September 7 and September 10, 2017, a strong enhancement in the proton intensities was observed by Advanced Composition Explorer (ACE) and WIND at L1 and Van Allen Probes, GOES-15 and POES-19 in the Earth's inner magnetosphere. Below geosynchronous orbit, Van Allen Probes and POES-19 show that no significant proton flux was observed with energies ≤25 MeV on September 4, while the fluxes peaked 3 to 7-times during September 7 and by ~25 times during the third proton flux event on September 10, 2017. Van Allen Probe-A observation shows that the closest distance that solar proton fluxes could approach the Earth is L~4.4 for 102.6 MeV energies on 10^{th} September 2017, while lower energy protons i.e., 25 MeV are observed deep up to L~3.4 on 11^{th} September 2017. POES-19 observations show that there is no particular magnetic local time (MLT) dependence of the solar proton flux and is symmetric everywhere at high and low latitudes. The measurements from multiple spacecrafts located in the different regions of the Earth's magnetosphere show that the increased level of solar proton flux population persisted for ~2 days. Thus, we quantify the temporal flux variability in terms of L-value, energy and MLT.

Plain Language Summary During a solar energetic particle (SEP) event, energetic electrons and ions flood the heliosphere causing severe damage to satellites, radio communication and humans in space. The Earth's magnetic field controls the dynamics of these particles to near-Earth space. One such unique event was observed in September 2017 for which the energy spectra and quantification of the proton fluxes spanning from 1.5 to 433 MeV using multi-satellite observations is studied. This was the largest proton event of the solar cycle 24 with three M-class and four X-class flares were observed by near-Earth spacecrafts. Proton fluxes were quantified at different locations like L1 point, geostationary orbit, inner magnetosphere, and low altitudes. The extent of flux enhancements, its access into the Earth's magnetosphere, MLT dependence and time to reach maximum fluxes are computed and compared before and after the SEPs arrived. We show that the multiple spacecraft observations are the key tool to quantify the temporal flux variability in terms of L-value, energy and MLT.

1. Introduction

It is widely accepted that there are two classes of solar energetic particle (SEP) events: (a) Impulsive SEP events, which are connected with a large solar flare (Miller, 1997) and (b) Gradual SEP events, which are responsible for diffusive shock acceleration associated with fast coronal mass ejections (CMEs) (Cane et al., 1991; Yan et al., 2006). CMEs are energetic ejections of coronal material weighing up to ~10^{17} g and speeds often exceeding 2,000 km/s into the heliosphere (see, e.g., Gopalswamy et al., 2016). Thus, CMEs and flares are two manifestations of the same magnetic energy release process when solar magnetic reconnection occurs (Wang et al., 1996; Zhang et al., 2001). Both CMEs and flares result in particle acceleration in the heliosphere that constitute an SEP event at the Earth. However, which process dominates the particle acceleration is still not clear (Li et al., 2009; Le et al., 2012; Qin & Shalchi, 2009). The early September 2017 solar proton events followed by a geomagnetic storm were well-studied using space and ground-based instruments (e.g., Gopalswamy et al., 2018; Sharykin & Kosovichev, 2018; Sun & Norton, 2017; Warren et al., 2018). The extreme solar activity during the first half of September 2017 is related to the Active Region NOAA 12673, which rapidly developed on 4^{th}-5^{th} September when near central meridian (e.g., Sun &

Table 1
List of Solar Flares (>M5 Class) Originated From Active Region 12673 During September 2017

Date	Flare (Class)	Flare (Peak time)	Halo CME
September 4	**M5.5**	**20:33**	**Yes**
September 6	X2.2	09:10	No
September 6	**X9.3**	**12:02**	**Yes**
September 7	M7.3	10:15	No
September 7	X1.3	14:36	No
September 8	M8.1	07:49	No
September 10	**X8.2**	**16:06**	**Yes**

Note. Data in bold text indicates the three solar energetic particle events registered at Earth by GOES-15 satellite. During these three events the proton fluxes are ≥10 pfu (1 pfu = 1 particle/cm^2-s-sr) for energies >10 MeV.

Norton, 2017) and rotated over the west limb on 10th September. Table 1 enlists several bright eruptions that were registered by GOES-15 satellite during 4-10th September 2017 with M-class and X-class flares (ftp://ftp.swpc.noaa.gov/pub/warehouse/). Solar proton event alerts are issued by the National Oceanic and Atmospheric Administration (NOAA) Space Weather Prediction Center. It is based on >10 MeV integral fluxes that are reported on a 5 min cadence after the fluxes have remained above a set level for three consecutive 5 min averages. Data in the bold text indicates the three major solar flares (https://cdaw.gsfc.nasa.gov/CME_list/sepe/) that were associated with fast CMEs and resulted into SEP events at Earth (Bruno et al., 2019). During three major SEP events particle intensity in the E > 10 MeV proton channel exceeds 10 particles/cm^2-s-sr. For each event, the flare class, peak time (UT) are shown, based on the Geostationary Operational Environmental Satellites-15 (GOES-15) X-ray archive (ftp://ftp.ngdc.noaa.gov/STP/space-weather/solar-data/solar-features/solar-flares/x-rays/goes/ along with the projected angular width of the associated CME ((https://cdaw.gsfc.nasa.gov/CME_list/).

A relatively high intensity (>100 MeV) proton fluxes were observed during September 10–14, 2017 causing a huge solar proton event that can adversely affect the sensors on-board spacecrafts and pose radiation hazards to the astronauts in space (Koons & Fennell, 2006; Moldwin, 2008; Snyder, 1967). The peak of three major flares that resulted into solar proton events at Earth were observed on 4th September at 20:33 UT, 6th September at 12:02 UT and 10th September, 2017 at 16:06 UT. A first, small SEP event with peak proton flux of 210 pfu is observed on September 4, 2017 at 19:20 UT https://www.ngdc.noaa.gov/stp/satellite/goes/doc/SPE.txt that originated from the moderately intense flare (M5.5). The peak time of a SEP event is the time when the integral flux of the >10 MeV protons reaches the peak value. The coordinated data analysis workshops (CDAW; https://cdaw.gsfc.nasa.gov/CME_list/) catalog of the Large Angle and Spectrometric Coronagraph (LASCO) onboard the Solar and Heliospheric Observatory (SOHO) indicates an erupted halo CME on the same day. The subsequent SEP event was associated with the X9.3 class flare, the largest flare in more than 10 yr (since December 2006) and the most intense in cycle 24. The flare peaked on September 6 at 12:02 UT with a halo CME and peak proton fluxes of 844 pfu on September 7, 2017 at 23:25 UT. Lastly, a third large SEP event occurred with the peak proton flux of 1,490 pfu on September 11, 2017 at 11:40 UT. It originated from another exceptional flare with X8.2 class peaking on September 10, 2017. This is the second largest soft X-ray flare of cycle 24 and was linked with a fast asymmetric halo CME in the CDAWcatalog.

Recently, O'Brien et al. (2018) studied >60 MeV protons using the Relativistic Electron-Proton Telescope (REPT) instrument on-board Van Allen Probes to analyze the particle access to higher altitudes and its dependence on energy and direction. They showed that compared to cutoff models, low-altitude proton measurements are far superior for near real-time monitoring of the geomagnetic cutoff. Moreover, Bruno et al. (2019) provide an assessment of SEP spectral shape in the entire range of energies from few hundreds of keV to a few GeV and explain the role of diffusive shock acceleration and other important external influences related to interplanetary transport and magnetic connectivity for the observed spectral break. However, they did not quantify the energy, L-value, and magnetic local tiime (MLT) that gets affected in response to the variability on the Sun. In this article, we make a quantitative approach of the proton flux measurements in the near-Earth region using multi-point observation. Such quantitative studies are very helpful in designing of the sensor threshold, damaging which could degrade the instrument and underestimate the incoming particle flux making it unusable for scientific studies. Quantitative analysis of proton fluxes is becoming more and more important as it is directly linked with solar activity. The objective of our study is to quantify the energetic protons access in the different regions in the Earth's magnetosphere using multi-satellite observations. We record the proton flux quantity, arrival time near the Earth, extent of penetration and its peak value into the Earth's magnetosphere by observing the major solar flare that occurred during September 4–10, 2017. As the spacecraft like ACE, WIND, Van Allen Probes, GOES-15, and POES-19 are located in the different regions of the Earth's magnetosphere, we could simultaneously scan the spatial and temporal characteristics of the radiation belt protons, at different energies. Quantitative analysis

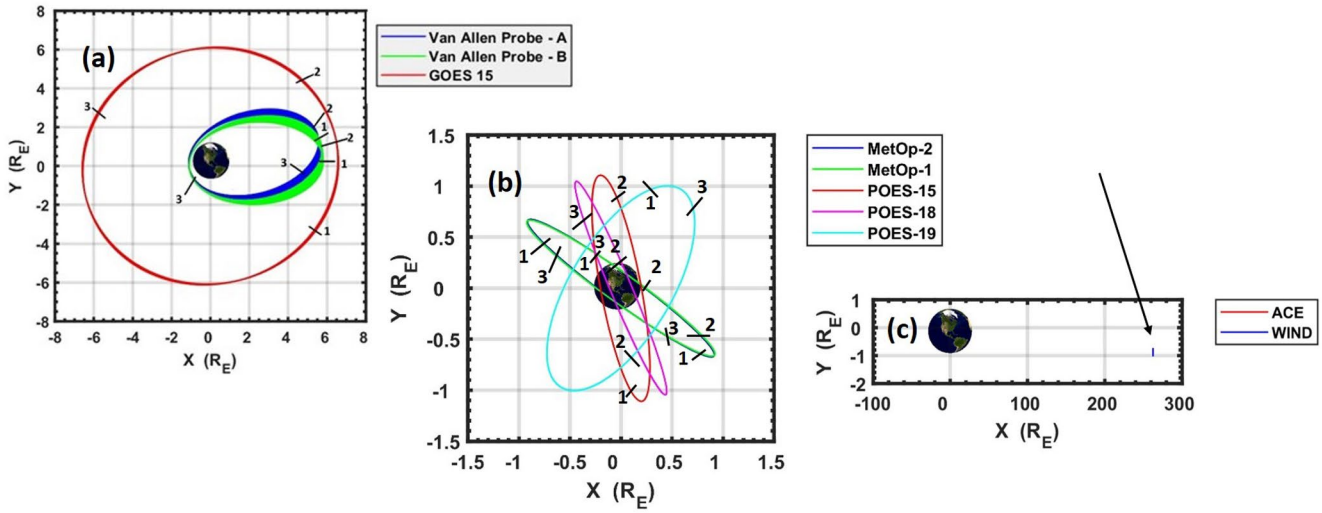

Figure 1. X-Y Plane view of the motion of (a) Van Allen Probe-A, Van Allen Probe-B, and GOES-15 satellites around the Earth in Geographic Solar-Magnetic (GSM) coordinates during September 2017. Blue, green, and red color give the trajectories of Van Allen Probe-A, Van Allen Probe-B, and GOES-15 satellites. (b) Orbit of MetOp-2 (blue), MetOp-1 (green), POES-15 (red), POES-18 (magenta), and POES-19 (Cyan). (c) Position ACE (red) and WIND (blue). The dashed black lines indicate the location of spacecrafts during the onset of first, second and third solar proton events observed at the Earth. Note: not to scale size of the Earth in panels (b, c).

provides the information in advancing intervals from time to time as multiple satellites lie into the different regions of the Earth's magnetosphere. The article is organized in the following manner: spacecraft data and September 2017 event are introduced in Section 2; in Section 3, we analyze various spectral solar proton flux measurements, the Phase Space Density (PSD) profiles and MLT dependence to identify the access and peak values of the proton flux during the event. Section 4 discusses the analyzed spectra and summary from our studies.

2. Satellite Data

Energetic particle flux measurements from mainly three different spacecrafts analyzed these events. These group of satellites include two Van Allen Probes (Probe-A, Probe-B) and POES-19. Here, we check the observations from all POES satellites like MetOP-1, MetOP-2, POES-15, POES-18, and POES-19 (but arbitrarily choose to show only POES-19 observations as an example) before concluding our results. Here, the observations are primarily reported by Advanced Composition Explorer (ACE), WIND, and GOES-15 spacecrafts. ACE and WIND measurement give the proton flux at Earth's L1 point, while Van Allen Probes and GOES-15 satellites provide proton distribution in the near-equatorial inner magnetosphere, while high energy precipitating protons at low altitude are measured using POES-19 spacecraft. Figure 1a gives the X-Y projection of Van Allen Probe-A (blue), Van Allen Probe-B (green), and GOES-15 (red) satellites; Figure 1b gives the orbit of all the POES satellites i.e., MeyOp-2 (blue), MetOp-1 (green), POES-15 (red), POES-18 (magenta), and POES-19 (Cyan) that revolves at an altitude of ~800 km; Figure 1c gives the position ACE (red) and WIND (blue) satellites that are located at the L1 point during September 2017. The location of each spacecraft during the onset of first, second and third solar proton events are marked by 1,2, and 3. The location of ACE and WIND is in the halo orbit and hence, we do not mark its position in panel (c).

Launched in August 2012, the Van Allen Probes (formerly known as the Radiation Belt Storm Probes) mission includes two identical observatories flying in highly elliptical orbits around the Earth with 1.1 × 5.8 R_E and inclination 10° (Baker et al., 2012; Mauk et al., 2012). Van Allen Probe-A and Van Allen Probe-B flies through different parts of the radiation belts at the same time, the data returned from the instruments can be combined to provide information about how the environment changes in both space and time (Kirby et al., 2012). Each Van Allen Probes observatory carries four suites, of which we have used Energetic Particle, Composition, and Thermal Plasma Suite-REPT (Stratton et al., 2012). REPT comprises of eight energy channels of proton flux covering the energy range from 20 to >100 MeV (Stratton et al., 2012). The

NOAA manages a constellation of geostationary and polar-orbiting spacecrafts. The NOAA GOES mission consists of a number of geosynchronous orbit satellites, of which we are particularly interested in the satellite that measures solar particle flux. Each GOES 13-15 satellite carries a pair of particle flux detectors, one looking eastward and one looking westward. However, the orientation of GOES-13 particle flux detector is fixed, while GOES-15 undergoes a yaw-flip twice a year at the equinoxes. Thus, it is possible for GOES-15 to relate the east-west effects of the particle flux with the eastward and westward looking detectors (Rodriguez et al., 2014). GOES-15 was launched in March 2010 and replaced GOES-11 in December 2011. For the present study, we use Energetic Proton, Electron, and Alpha Detectors (EPEADs) onboard GOES-15 satellite, as it provides 1 min resolution data of proton fluxes at seven energy channels in the range of our interest (i.e., 0.74–900 MeV; GOES, 2010). Contrary to geosynchronous measurements, the low-altitude measurements are made using NOAA POES mission that consists of a number of polar-orbiting satellites operating simultaneously with good coverage over a broad range of MLT and L-value ∼2–8 every ∼100 min. As a polar-orbiting sun synchronous satellites at an altitude of ∼800 km with a ∼98.5 inclination, the POES satellites carry a newer and modified SEM (Space Environment Monitor) called SEM-2 instrument package that includes various particle detectors. MetOp (Meteorological Operational Satellite Program of Europe) is Europe's first polar-orbiting (LEO) satellite that carries NOAA-provided instrument package SEM-2. In the present studies, 2 s resolution omni-directional proton differential flux at three different energy channels (25, 50, and 100 MeV) are analyzed using Medium Energy Proton and Electron Detector onboard EUMETSAT's MetOp-1, MetOp-2 and POES-15, POES-18 and POES-19 satellite (Evans & Greer, 2000; Green, 2013). The data is available under https://satdat.ngdc.noaa.gov/sem/poes/data/. The differential fluxes at 25, 50, and 100 MeV are derived from a piecewise spectral fit of the four original omni, integral sensor outputs covering the range from 16 to 250 MeV (Machol, 2012; Redmon et al., 2015)

ACE was launched into halo orbit at Earth's first Lagrangian (L1) point on August 25, 1997. Of numerous instruments on-board ACE spacecraft, we use electron, proton, and alpha monitor (EPAM; Gold et al., 1998) that is specifically designed to measure ions ($E > 40$ keV) from five separate solid-state detector telescopes oriented to give nearly 4π angular coverage. ACE-EPAM comprises of low energy magnetic spectrometer LEMS30 and LEMS120 sensors pointing at 30° and 120°, respectively, from the Sunward-pointing spin axis, which measures the ion flux from 46 keV to 4.8 MeV with 5 min resolution (Zwickl et al., 1998; http://www.srl.caltech.edu/). A spin-stabilized WIND spacecraft was launched at the same location as the ACE spacecraft to give the measurements of solar wind before it interacts with the Earth's geomagnetic field. WIND Energetic Particles: Acceleration, Composition consists of various telescope systems of which we used ELectron-Isotope TElescope system that comprises of two Alpha-Proton-Electron telescopes that measure the proton flux with 92 s resolution in the range 19–28 MeV/n and 28–72 MeV/n (Von Rosenvinge et al., 1995).

3. Observations and Analysis

Figures 2a–2d show the proton flux measured in the halo orbit at L1 point, while panel (e) represents Sym-H, during August 25 to September 30, 2017. The black dashed vertical lines (1, 2, and 3) correspond to the onset time of enhancement in the proton intensities during three major flares (Bold text in Table 1). The pink-dotted vertical lines indicate the three interplanetary shocks that passed by during this interval. Sym-H index represents the intensity of the magnetic storm (panel e) and is obtained from NASA's CDAWeb (http://cdaweb.gsfc.nasa.gov/). It is derived using 1 min values from a different set of stations than those used for the derivation of Dst (they are not simply 1 min versions of the Dst index; Iyemori & Rao, 1996). Energetic proton accelerated by the flare travel out from the Sun and cross the geomagnetic field lines when directed toward the Earth. (Birch et al., 2005) showed that the equatorward displacement of the invariant latitude of the cutoff in proton flux was found to be strongly correlated with the magnetic storm indices (Sym-H). The first shock is indicated by a minor geomagnetic storm (panel e) at 23:43 UT on September 6. It was driven by CME observed by SOHO/LASCO on September 4 and associated with the first SEP event. A subsequent shock observed at 23:00 UT on September 7 (based on the storm sudden commencement time) was associated with the CME observed by SOHO/LASCO on September 6 at 12:24 UT that was also associated with the second SEP event. Lastly, the third shock was associated with September 10 SEP event. Since we focus to study the Earth-directed SEPs due to major flares, we analyze the proton events marked with 1, 2,

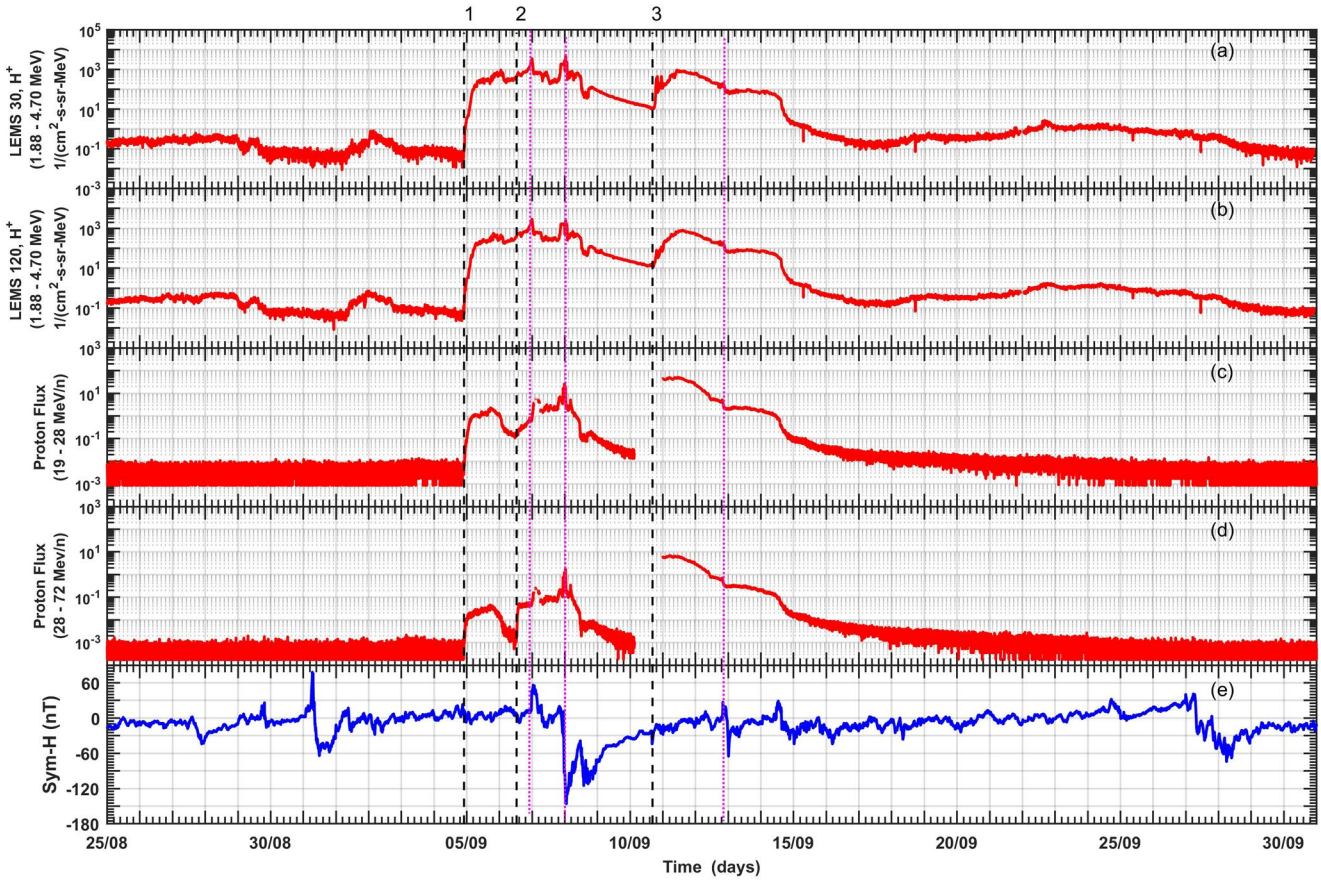

Figure 2. The proton flux measurements from LEMS 30 and LEMS 120 instruments on-board ACE (panels (a, b)) and WIND-EPAM observations in the energy range 19–28 MeV/n and 28–72 MeV/n (panels (c, d)) are shown for the period from August 25 to September 30, 2017. Panel (e) represents Sym-H. Three dashed vertical lines correspond to the onset time of enhancements in the proton intensities during three major flares.

and 3. The vertical lines at 1, 2, and 3 indicate the onset time of the proton fluxes on September 4 at around 22:00 UT, around 12:25 UT on September 6 and around 16:05 UT on September 10, respectively. Panels (a, b) show a clear two peaked proton fluxes in the energy range of 1.88–4.70 MeV measured by LEMS 30 and LEMS 120 instruments onboard ACE. In both LEMS sensors, the proton fluxes enhanced from ~10^{-1}/cm^2-s-sr-MeV (on September 4) to 10^3/cm^2-s-sr-MeV (on September 10) and continued to be high till September 15, 2017. A continuous injection of <5 MeV protons were observed for nearly 12 days. Panels (c, d) represent the WIND-EPAM observations of proton fluxes in the higher band of energies i.e., 19–28 MeV/n and 28–72 MeV/n, respectively. A sharp increase of the order of about three is observed from September 4 to September 10, 2017 on both the telescopes, while observed data gap in panels (c and d) are due to sensor saturation. Before the first solar flare event on September 4, 2017, the proton fluxes were ~ 10^{-2}/cm^2-s-sr-MeV and ~ 10^{-3}/cm^2-s-sr-MeV in the energy band of 19–28 MeV/n and 28–72 MeV/n, respectively. The detailed quantification of proton fluxes for each event is given in Tables 2–4. Table 2 gives the overview of the proton fluxes during the first solar proton flux event, that were observed by various satellites in the different band of energies, L-value and MLT. The corresponding start time (T*i*), peak time (T*p*) and end time (T*e*) of the proton fluxes are shown along with its corresponding flux values during start time (F*i*), peak time (F*p*) and end time (F*e*). Similarly, Tables 3 and 4 gives the information of the proton flux change during second and third solar proton events, respectively.

The temporal variation of the particle measurements observed by ACE and WIND necessitates the investigation of proton flux dynamics recorded by various space-borne measurements present in the Earth's magnetosphere. Hence, we obtain the Energy-Time (E-T) spectrogram of proton flux measured by multiple spacecrafts in the wide range of energies during September 4–15, 2017. Figures 3a and 3b give the

Table 2
The Table Gives the Overview of the Proton Fluxes During the First Solar Proton Event That Occurred on September 4, 2017

Spacecraft	Energy (MeV)	*L*-value	MLT (hh:mm)	T*i*	*Fi*	*Tp*	*Fp*	*Te*	*Fe*	*Fp*/*Fi*
ACE	1.88–4.70 (LEMS-30)	L1 point	~12:00	2017/09/04 21:18	0.01201	2017/09/06 01:06	392.1	2017/09/06 07:30	281.6	3.26e + 04
ACE	1.88–4.70 (LEMS-120)	L1 point	~12:00	2017/09/04 21:18	0.03077	2017/09/05 19:36	552.3	2017/09/06 07:30	204.5	1.79e + 04
WIND	19–28	L1 point	~12:00	2017/09/04 21:48	0.002585	2017/09/05 17:42	2.251	2017/09/06 6:42	0.1489	870.79
Van Allen Probe - B	21.25	5.3	11:35	2017/09/05 18:49	1.2048	2017/09/05 19:33	1.9503	2017/09/05 20:58	1.3360	1.6188
GOES-15	30.6	6.6	07:57	2017/09/04 22:40	0.04599	2017/09/05 07:24	1.403	2017/09/06 10:24	0.1905	30.5

Note. Various satellites in the different bands of energies, L-value and MLT. The corresponding start time (T*i*), peak time (T*p*), and end time (T*e*) of the proton fluxes are shown along with its corresponding flux enhancement during start time (F*i*), peak time (F*p*), and end time (F*e*). The quantifying ratio of the peak proton flux to initial proton flux is given for each observation made by spacecraft. During the first solar proton flux event, Van Allen Probe-A and POES-19 satellites do not record any significant change in fluxes and are hence not listed in the table.

spin-averaged proton flux measured by Van Allen Probe-A and Van Allen Probe-B, panel (c) POES-19 proton flux in 25, 50, and 100 MeV (d) proton flux from the westward-viewing EPEAD onboard GOES-15; seven energy channels (P1-P7) spanning the nominal range 2.5–433 MeV energy channels. Panels (e, f, g) show the corresponding solar wind parameters like solar wind velocity (*V*sw), dynamics pressure (*P*sw) and IMF *B*z, respectively. To know about the interplanetary characteristics of the space weather events, the solar wind plasma and IMFs were obtained from the NASA's CDAweb. The lowest panel of Figure 3 gives the Sym-H index with the minimum of −146 nT at 0107 UT on September 8, 2017. The pink-dashed vertical lines are same as the black dashed lines in Figure 2. Panels (a–d) show no major proton fluxes over 20 MeV during the first solar proton event i.e., on September 4, 2017. Contrarily, on September 7, 2017, a slight increase in proton flux was observed by Van Allen Probe-A and Van Allen Probe-B (panels (a, b)) in the energy range of 21.25–27.6 MeV and continued for ~24 h in both the probes. Further, a much stronger

Table 3
This Table Is Same As Table 2 That Gives the Information of the Proton Flux Changes but During Second Solar Proton Event That Occurred on September 7, 2017

Spacecraft	Energy (MeV)	*L*-value	MLT (hh:mm)	T*i*	*Fi*	*Tp*	*Fp*	*Te*	*Fe*	*Fp*/*Fi*
ACE	1.88–4.70 (LEMS-30)	L1 point	~12:00	2017/09/06 08:12	279.6	2017/09/06 23:30	3,437	2017/09/07 01:18	659.9	12.2926
ACE	1.88–4.70 (LEMS-120)	L1 point	~12:00	2017/09/06 05:42	204.5	2017/09/06 23:12	2,375	2017/09/06 23:52	1570	11.6137
WIND	19–28	L1 point	~12:00	2017/09/06 10:18	0.1431	2017/09/07 01:18	3.623	2017/09/07 05:54	3.8036	25.3180
Van Allen Probe - A	21.25	5.5	13:23	2017/09/07 01:58	1.0704	2017/09/07 03:56	7.7965	2017/09/07 04:36	1.3360	7.2837
Van Allen Probe - B	21.25	5.6	12:10	2017/09/07 07:41	1.1171	2017/09/08 07:30	7.9651	2017/09/07 04:42	1.3744	7.1301
GOES-15	30.6	6.6	14:39	2017/09/06 11:12	0.1314	2017/09/07 04:18	2.047	2017/09/07 18:54	1.175	8.9422
POES-19	25	4.8	14:47	2017/09/06 13:08	0.5835	2017/09/07 03:42	3.24	2017/09/07 06:22	1.063	5.5527

Table 4
This Table Is Same As Table 2 That Gives the Information of the Proton Flux Changes but During Third Solar Proton Event That Occurred on September 10, 2017

Spacecraft	Energy (MeV)	*L*-value	MLT (hh:mm)	*Ti*	*Fi*	*Tp*	*Fp*	*Te*	*Fe*	*Fp/Fi*
ACE	1.88–4.70 (LEMS-30)	L1 point	~12:00	2017/09/10 17:06	11.48	2017/09/11 12:06	827	2017/09/12 21:24	114	72.03
ACE	1.88–4.70 (LEMS-120)	L1 point	~12:00	2017/09/10 17:24	13.39	2017/09/11 15:12	763.5	2017/09/12 15:48	191	57.02
WIND	19–28	L1 point	~12:00	–	–	2017/09/11 12:36	48.23	2017/09/13 02:30	2.385	–
Van Allen Probe - A	21.25	3.2	10:45	2017/09/10 17:54	1.1145	2017/09/11 14:12	24.4906	2017/09/13 01:00	1.0970	21.9745
Van Allen Probe - B	21.25	5.6	03:58	2017/09/10 17:48	1.1306	2017/09/11 11:36	25.7632	2017/09/13 01:30	2.4502	22.7871
GOES-15	30.6	6.6	22:68	2017/09/10 17:24	0.03641	2017/09/10 18:42	36.13	2017/09/12 13:06	5.148	992.3098
POES-19	25	4.8	03:27	2017/09/10 17:54	1.524	2017/09/10 21:48	25.77	2017/09/14 12:36	1.89	16.90

Note. The blank columns corresponding to the WIND observations (T*i* and F*i*) refers to the time where a data gap is observed (see Figure 2).

enhancement of proton flux in the energy range of 21.25–102.6 MeV was observed by Probe-A and B on September 10, 2017. Similar enhancements were also evident in POES-19 (panel c) and GOES-15 (panel d) present at different locations in the wide range of energies.

To quantify the flux enhancement at different L-values, we represent the spin averaged differential proton flux in terms of *L*-value versus time (*L*-T) spectra from September 4–15, 2017. Figure 4 shows the proton fluxes measured by Van Allen Probe-A (a1–a3), Probe-B (b1–b3), and POES-19 (c1–c3) satellite for three different band of energies i.e., ~25 MeV (left), ~50 MeV (center) and ~100 MeV (right). The pink dashed vertical lines are same as in Figure 3, while Figure 4e represents the Sym-H component (same as Figure 3h). Panels (a1, b1) show that on September 4, there was no observable proton flux intensification for $L > 2.5$ and remained as low as 10^{-1}-10^{-2}/cm^2-s-sr-MeV. However, on September 7, at L ~5 and $E = 21.25$ MeV the proton flux observed by Van Allen Probe-A and B were ~1–3/cm^2-s-sr-MeV that enhanced to ~10/cm^2-s-sr-MeV on September 10 and diminished on September 14, 2017. Panel (c1) refers to the POES-19 proton fluxes in the lowest band of energies i.e., 25 MeV. A slight proton flux enhancements are observed during September 4–6 with a strong enhancements on September 7, 2017. The proton flux values in the L ~1–20 is about 5/cm^2-s-sr-MeV with even stronger enhancements during third solar proton event i.e., on 10th September. The integral flux across all the *L*-values rises to ~20/cm^2-s-sr-MeV, which is about five times the flux observed on 7th September. Similar tendencies were observed at higher energies for all the spacecrafts as shown in Figure (a2–c2 and a3–c3). However, the higher energy (~50 MeV and ~100 MeV) fluxes appeared only during third solar proton event for all the spacecrafts.

3.1. Accessibility in the Earth's Magnetosphere

To know the extent of proton flux accessibility in the Earth's inner magnetosphere, the PSD is calculated. To calculate relativistic electron PSD, a method based on the studies of Chen et al. (2005) and Turner and Li (2008) is employed. The differential proton flux (j), at a given energy (E) and time (t) is converted to PSD (f), using the following equation:

$$f = 3.325 \times 10^{-8} \frac{j(E)}{E(E + 2m_0c^2)} \left[\left(\frac{c}{MeV.cm} \right)^3 \right] \quad (1)$$

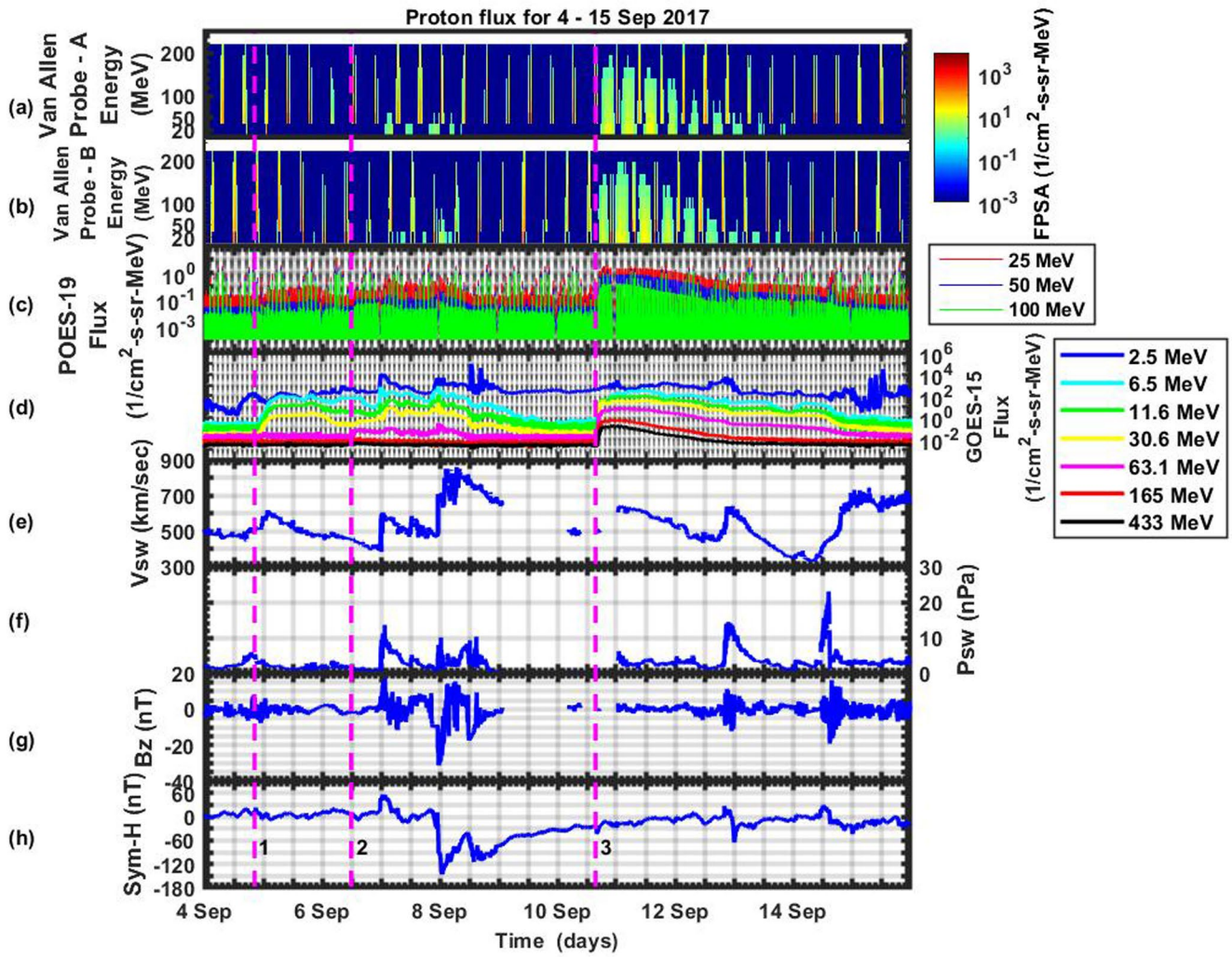

Figure 3. The Energy-Time (E–T) spectrogram of proton flux measured by (a) Van Allen Probe-A and (b) Van Allen Probe-B in the energy range of 20–200 MeV for September 4–15, 2017. Panels (c, d) proton fluxes measured by POES-19 and GOES-15 Satellites, respectively. Panels (e, f, g) give the solar wind parameters like *V*sw, *P*sw, and IMF *B*z. The lowest panel (h) gives the Sym-H index with Sym-H minimum.

where j is the proton flux in particles/cm^2-sr-s-keV, E is the proton's kinetic energy in MeV, m_0c^2 is the electron rest mass in MeV, and the numerical factor converts to the units shown in brackets.

The observation of proton flux at L1-point (using ACE and WIND satellite) and geosynchronous orbit (GOES) gives information of the quantity of incoming flux and its peak time for >6.6 R_E. The spacecrafts like ACE, WIND, and GOES-15 do not record proton fluxes into and out of the Earth's inner magnetosphere, hence we utilize observations made by only Van Allen Probes. To know the access of proton flux in the near-Earth region (<4 R_E), the observations from Van Allen Probes are analyzed, while MLT dependence is analyzed using POES-19 Satellite shown in Figure 6. Figure 5 shows the PSD profile as a function of L-Shell. The proton flux measurements from Probe-A and B are shown in two distinct sections of Figure 5, left and right, respectively. Each separate panel corresponds to one orbit of Van Allen Probes. The outbound and inbound passages of the Probes are indicated by dotted and solid lines, respectively. Proton PSD at different energies are represented by colored scale. The top three panels on each side (i.e., a1–a3 and b1–b3) show the interval of the first solar proton flux event. During this event, only the inner belt protons are observed upto L ~2.5 with empty outer belt. The proton fluxes do not appear beyond $L > 2.5$ even on September 5–6, 2017 and hence not shown in the figure. However, during second solar proton event on 7th September 2017

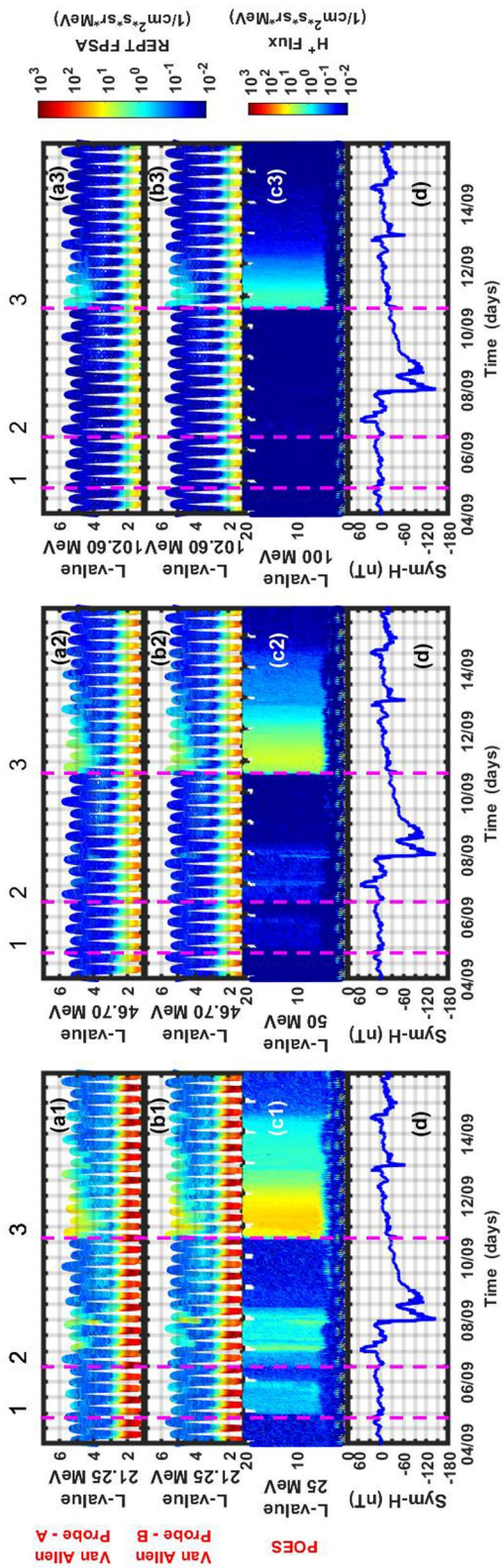

Figure 4. *L*-value versus Time (*L*-T) spectra obtained for differential proton flux from September 4–15, 2017 is shown for 3 different band of energies; ~25 MeV (left), ~50 MeV (center) and ~100 MeV (right). The proton fluxes measured by Van Allen Probe-A (panels a1–a3), Probe-B (panels b1–b3), and POES-19 (panels c1–c3). The lowest panel (d) represents Sym-H, while the pink dashed vertical lines represent the time of enhancements in the proton intensity during three different flares.

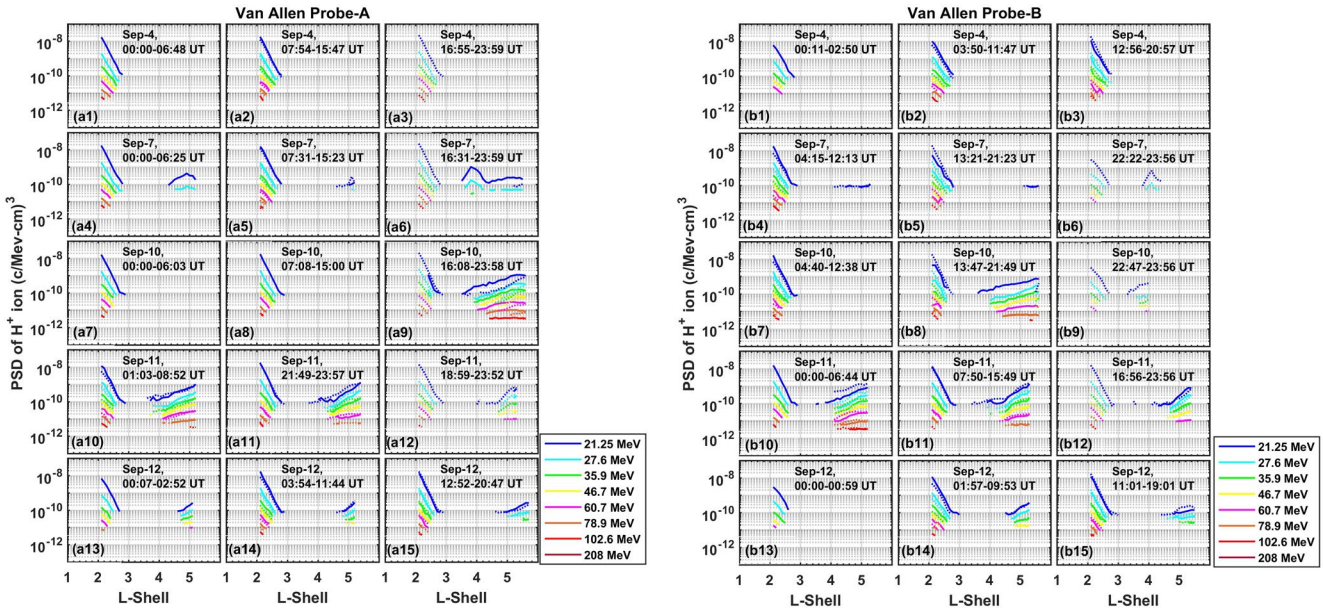

Figure 5. Phase Space Density (PSD) of protons measured by Van Allen Probe A (left-section) and B (right-section) is shown as a function of different *L*-values. Each color code represents the proton energy, available under the REPT instrument. Dotted and solid lines represent the outbound and inbound Passages, respectively. Top three set of panels in both spacecraft (a1–a3, b1–b3) show the interval of first solar proton flux i.e., 4^{th} September 2017. Panels a4–a6 and b4–b6 represent the duration of second solar proton event (i.e., 7^{th} September 2017) while, panels a7–a9 and b7–b9 represent the duration of third solar proton event (i.e., 10^{th} September 2017). Panels a10–a15 and b10–b15 show the duration after solar proton fluxes are injected.

(panels a4–a6, b4–b6), the energetic protons appear on higher *L*-shells. The fluxes as close as L ~3.5 are observed on September 7 from probe-A (panel a6).

Proton fluxes diminish on 8^{th} September (not shown). However, they reappear at higher *L*-shells ($L > 3$) on 10^{th} September during third solar proton event in both the Probes. Probe-B was located at right place to record the initial proton access into the Earth's inner magnetosphere (panel b8), while Probe-A records it later in time. A very high energy proton flux is observed across all the energies ranging from 21.25 to 102.6 MeV. The proton flux continues to be at high even the following day (i.e., on 11^{th} September 2017) that diminishes lately on September 11–12, 2017 in the different band of energies. During last two solar proton flux events, the proton flux accessibility is observed quiet deep into the Earth's inner magnetosphere. During third solar proton event i.e., on 10^{th} September 2017, the protons with 21.25 MeV were observed up to L~3.6 from Probe-A (panel a9), while it is observed as close as L~3.4 using Probe-B (panel b10).

3.2. MLT Dependence

To identify the MLT dependence of the proton fluxes in the Earth's inner magnetosphere during the proton flux event, the satellite must revisit and trace the same orbital path in a very short interval of time. This is difficult to achieve with geostationary satellites like GOES-15 (having the orbital time of ~24 h) or highly elliptically orbiting Van Allen Probes (having the orbital period of ~9 h). However, this study is possible using LEO satellites like POES-19 that quickly spans across different MLTs making it possible to know its time of peak flux. The proton flux from POES-19 spacecraft as a function of *L*-value at different times is shown in Figure 6. Three separate sections (i.e., panels a–f, g–l, m–r) correspond to three different energies 25, 50, and 100 MeV, respectively. The color code represents different MLT sectors. Overall, at any given period of time, the proton flux reduces as the energy increases across all the MLTs and *L*-values. POES-19 proton fluxes during second solar proton flux on 7^{th} September was ~5/cm^2-s-sr-MeV and diminished on 8*th* and 9*th*. Peak proton fluxes were observed at L~7, on 10*th* September 04:54 MLT (i.e., in the dawn sector). The similar results are checked using other POES satellites like Metop-1 and Metop-2, POES-15 and POES-18 and taken all its energy channels into account (not shown). The proton fluxes as high as ~35/cm^2-s-sr-MeV

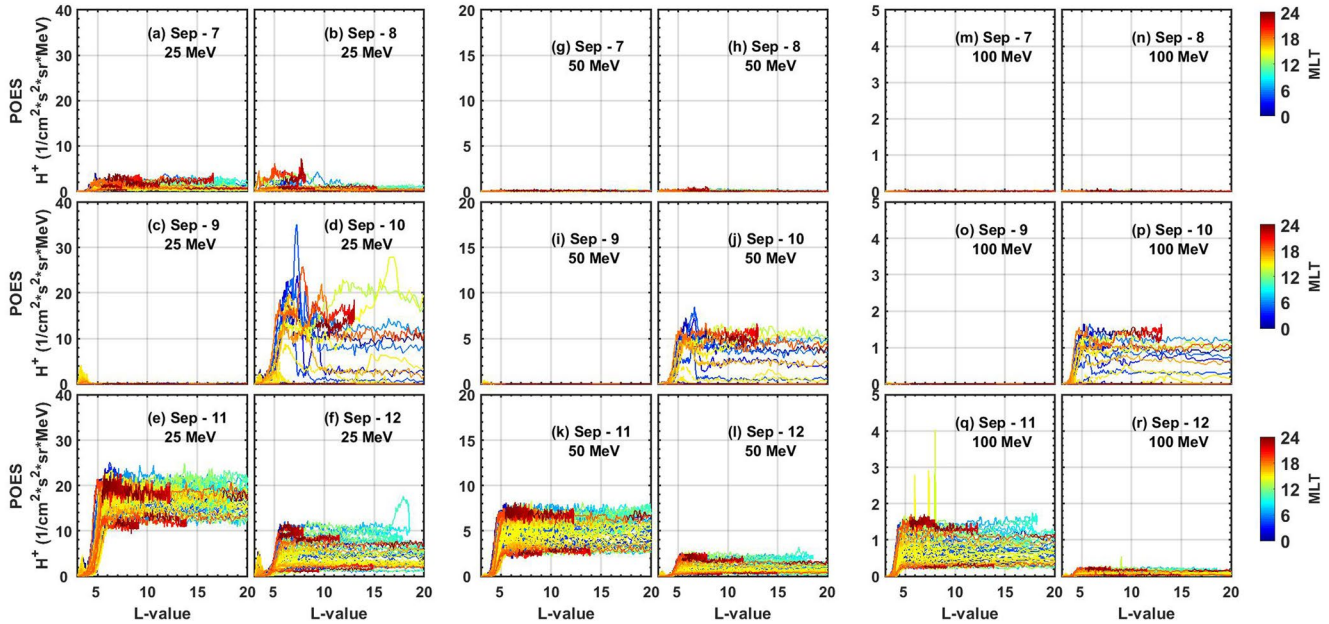

Figure 6. Proton flux measured by POES-19 spacecraft as a function of *L*-value for (a–f) 25 MeV, (g–l) 50 MeV, (m–r) 100 MeV is shown. The color code represents the MLT sectors covered by POES-19. Each panel represents the duration of one day.

were observed at 25 MeV with a simultaneous peak in 50 and 100 MeV energies. Peak proton fluxes persisted for about 2 days with no particular dependence and constant flux values across all the MLT sectors.

4. Discussion and Summary

An exceptional interval of solar activity with the large number of bright eruptions, including four X-class flares were observed between September 4 and 15, 2017 during the late declining phase of solar cycle 24 (see Table 1). A solar proton event was detected during 4^{th} September that originated from the M5.5 class flare and ejected a CME. On the other hand, two strongest flares with X9.3 and X8.2 intensities are observed on 6^{th} September and 10^{th} September 2017, respectively. Both the solar proton flux events, measured by near-Earth spacecraft, are linked with the fast CMEs. The present study quantifies proton flux enhancement during the strongest solar proton event since December 2006. Tables 2–4 refer to the quantitative assessment of three major solar proton fluxes measured by various satellites in the different L-values and different bands of energies. The first column in Table 2 refers to the satellite that made the observation of proton flux changes during September 4, 2017. The energy channel, L-value and MLT that recorded the first flux enhancements are shown in column 2, 3 and 4, respectively. The corresponding start time (T*i*), peak time (T*p*) and end time (T*e*) of the proton fluxes is shown along with its corresponding flux enhancement during start time (F*i*), peak time (F*p*), and end time (F*e*). To quantify the extent of enhancement during each energy the ratio of the peak proton flux (F*p*) to initial proton flux (F*i*) are calculated in the last column for each observation made by spacecraft. During the first solar proton flux event, Van Allen Probe-A and POES-19 satellites do not record any significant enhancement in fluxes and is hence not listed in Table 2. The calculated ratio of the proton flux indicates a significant change in the proton fluxes at and beyond the geosynchronous orbit. However, only a small (less than double) flux enhancement is observed beyond $L = 5$ on September 5, 2017 using Van Allen Probe-B. Similarly, Tables 3 and 4 give the proton fluxes that are observed during September 7 and September 10, 2017, respectively. The data gap observed in Table 4 corresponds to the data gap observed by the WIND spacecraft on September 10, 2017. Multiple satellite observations from Tables 3 and 4 show that the proton fluxes increase by the factor of three or more from second to third solar proton flux event. To obtain the overall idea of the flux change over a wide range of energies, we analyze the energy-flux spectrogram for all the three events.

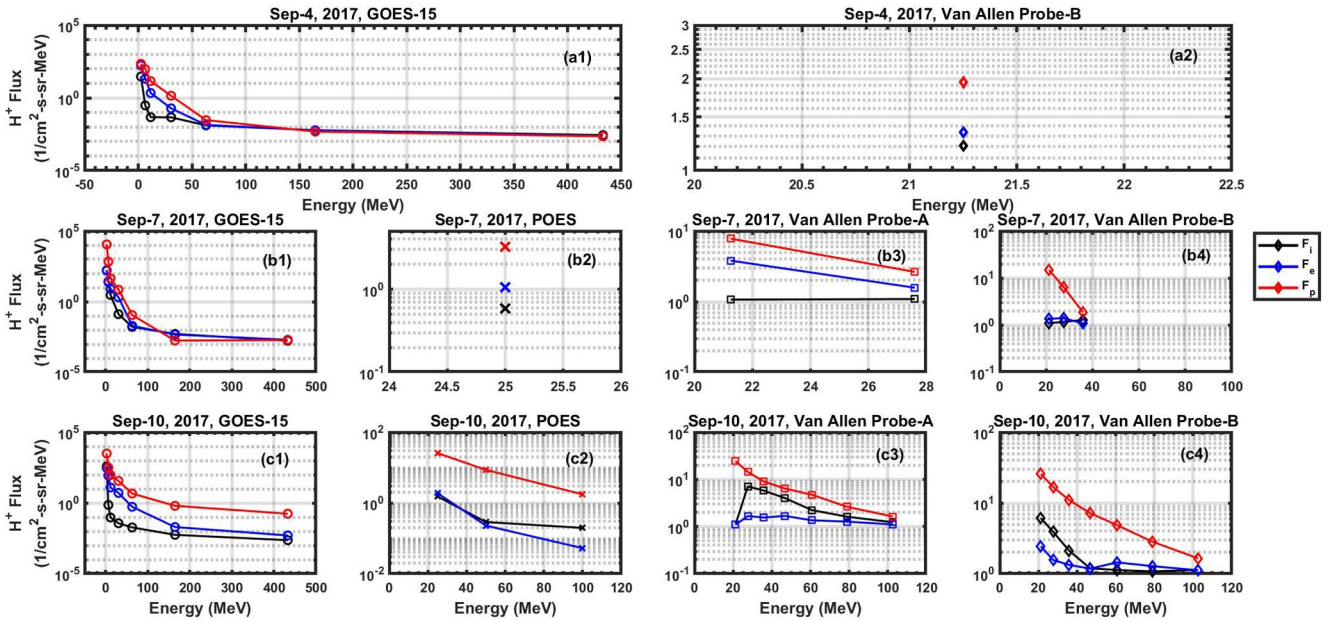

Figure 7. Energy flux versus energy range during three solar proton events using multiple satellites is shown. Panels (a1–a2) show the first proton flux event that occurred during September 4, 2017. Black, Blue, and Red curve indicate the fluxes during start time, end time, and peak time, respectively. On September 4, proton flux enhancements were observed in the inner magnetosphere by GOES-15 and Van Allen Probe-B. Similarly, panels (b1–b4) show the second proton flux event that occurred during September 7, 2017 and observed by GOES-15, POES-19, Van Allen Probe-A and Van Allen Probe-B, respectively. Panels (c1–c4) are same as panels (b1–b4) except for the third proton flux event that occurred during September 10, 2017.

Figure 7 shows the energy flux versus energy range for the three proton flux events that occurred during September 2017. We study the spectral hardening in the Earth's inner magnetosphere by using proton fluxes that are recorded in the large energy band by using various spacecraft measurements at different locations in the Earth's inner magnetosphere. Hence, we only focus on the observations made by satellites within the Earth's inner magnetosphere and ignore the observations made by ACE and WIND satellites at L1-point. Panels (a1–a2) show the proton fluxes recorded by GOES-15 and Van Allen Probe-B during September 4, 2017. Van Allen Probe-A and POES-19 do not show any significant fluxes during this period and hence we do not show it. Black, Blue, and Red curve indicate the fluxes during start time, end time, and peak time, respectively. Panel (a1) shows that the proton flux with the energies >10 to <50 MeV increases during its peak interval (red) and then recovers back to its initial value during the end of the event (blue). The magnitude of the change in proton flux is different at different energies. Similarly, panel (a2) shows the proton fluxes measured by Van Allen Probe-B at 21.25 MeV. The peak flux value (red) increases by less than double during this event. Similarly, panels (b1–b4) show the proton flux observations during September 7, 2017 using GOES-15, POES-19, Van Allen Probe-A and Van Allen Probe-B, respectively. A spectral hardening is observed for most of the energies in all the satellites. Panel b2 represents the proton flux change observed by POES-19 only at 25 MeV as the fluxes at higher energies like 50 MeV, 100 MeV does not appear. Similarly, panels (c1–c4) show the proton fluxes during September 10, 2017 using GOES-15, POES-19, Van Allen Probe-A and Van Allen Probe-B, respectively. It is interesting to compare the peak proton fluxes (red) using GOES-15 observations for September 7 and September 10 (i.e., panels b1 and c1) that shows not much difference in flux enhancements below ~20 MeV, while the deviation of the order of two or more is observed for the fluxes beyond 20 MeV. Similarly, different orders of the enhancement of fluxes are observed when we compare peak flux observations made by various satellites shown in panels b2–c2, b3–c3, and b4–c4.

Although the particles are not magnetically trapped at such high energies, the proton gyration makes it possible to observe its access at a given L-shell. O'Brien et al. (2018) showed that the finite gyroradius effect, coupled with L-shell, can be used to explain most of the energy dependence at high altitude. They observed that the deeper penetration of these energetic protons can lead to inverted spectra for certain L-values in the inner magnetosphere. However, the process that violates the third adiabatic invariant for trapped particles are important for populating the radiation belt. Earlier studies using IMP-8, ISEE-3 and

ACE extensively studied solar energetic protons that are accelerated due to shock wave from the event site (Dungey et al., 1965). Le and Han (2005) investigated the acceleration of SEP by CME-driven shock in interplanetary space based on the SEP data from ACE and GOES satellites. They showed that the acceleration process of SEP by the 2000 July 14 CME-driven shock ran through the whole space accelerating protons to >100 MeV. (Mewaldt et al., 2005) studied the period from late October through early November 2003 during which five large SEP events occurred. Using data from instruments on the ACE, SAMPEX, and GOES-11 spacecraft, they show that the proton fluences in the 28 October 2003 event are comparable to the largest observed during the previous solar maximum, and within a factor of two or three of the largest SEP events observed during the last 50 yr.

In summary, very high energy (>20 MeV) proton flux observation in the Earth's inner magnetosphere is focused using space-borne measurements from ACE, WIND, GOES-15, Van Allen Probes, and POES-19. Relativistic protons have extremely high energy and are those uniquely trapped particles in the Earth's magnetosphere which does not appear beyond L~2.5. ACE observations at L1-point distinctly mark the onset of each solar proton event with the flux increase of the order >3 on September 4 in 1.88–4.7 MeV energy channel. Similarly, WIND spacecraft marks the change of the order >2 in 19–28 MeV and >1 in 28–72 MeV on September 4. During this event, Van Allen probes made a very important and crucial observations of these most energetic radiation belt protons, deep into the inner magnetosphere. Moreover, the extent of proton access deep into the inner magnetosphere is thoroughly investigated. For example, Van Allen Probe observations show that there are no significant enhancement in the proton flux (double or more) beyond $L = 3$ for the first solar proton event (i.e., 4^{th} September 2017); for second solar proton event (7^{th} September 2017), the lower energies like (21.25–35.9 MeV) are observed deep upto L~3.8–3.4, with the lowest energies penetrated the most, while during the third solar proton event the proton flux penetrated upto L~3.4–4.4 with energies from 21.25 to 102.6 MeV. However, these fluxes diminish from the lower L-values first. The major summary from our studies are:

1. Below geosynchronous orbit, no significant proton flux was observed with energies ≤25 MeV on September 4, while the fluxes peaked 3 to 7-times during September 7 (Table 3: Van Allen Probes and POES-19 observations). In addition, the fluxes with energies ≤25 MeV enhanced by ~25 times below geosynchronous orbit, during the third proton flux event on September 10, 2017 (Table 4: Van Allen Probes and POES-19 observations)
2. Van Allen Probe measurements at $L = 5$ and $E = 21.25$ MeV shows that the proton flux is ~10.5/cm^2-s-sr-MeV and it persisted for ~48 h from September 10–12, 2017 (Figure 4)
3. To study the dynamics at low-Earth Orbit, POES-19 observations are utilized to know the proton flux dynamics during the solar proton event for 25, 50, and 100 MeV. A transient maximum flux is observed at L~7, with the flux value 34.99/cm^2-s-sr-MeV at 25 MeV energy channel at 0454 MLT, which remains same for 50 and 100 MeV energies
4. Van Allen Probe-A observation shows that the closest distance that solar proton fluxes could approach the Earth is L~4.4 for 102.6 MeV energies at 2010UT on 10^{th} September 2017, while lower energy protons i.e., 25 MeV are observed deep upto L~3.4 at 0436 UT on 11^{th} September 2017
5. POES-19 observations show that there is no particular MLT dependence of the solar proton flux and is symmetric everywhere at high and low latitudes

The measurements from multiple spacecrafts located in the different regions of the Earth's magnetosphere show that the increased level of solar proton flux population persisted for ~2 days and helped us to quantify the flux at different locations and energy range.

Data Availability Statement

NOAA-POES and GOES-15 data are from NOAA's National Center for Environmental Information at satdat.ngdc.noaa.gov. Solar wind IMF data and geomagnetic indices were obtained from the GSFC/SPDF OMNIWeb interface available at http://omniweb.gsfc.nasa.gov.

Acknowledgments
The authors sincerely thank Dr. Y. Ebihara for the constructive discussion throughout this work. The authors acknowledge S. G. Kanekal, D. N. Baker, and the entire team for processing and making the REPT data available on https://rbsp-ect.lanl.gov/rbsp_ect.php. The authors thank referees for their constructive comments which improved the manuscript. The authors thank the teams who created and provided the WIND and ACE plasma data used in this analysis.

References

Baker, D., Kanekal, S., Hoxie, V., Batiste, S., Bolton, M., Li, X., et al. (2012). The Relativistic Electron-Proton Telescope (REPT) instrument on board the radiation belt storm probes (RBSP) spacecraft: Characterization of Earth's radiation belt high-energy particle populations. In *The van Allen probes mission* (pp. 337–381). Springer. https://doi.org/10.1007/978-1-4899-7433-4_11

Birch, M., Hargreaves, J., Senior, A., & Bromage, B. (2005). Variations in cutoff latitude during selected solar energetic proton events. *Journal of Geophysical Research*, *110*(A7). https://doi.org/10.1029/2004ja010833

Bruno, A., Christian, E., de Nolfo, G., Richardson, I., & Ryan, J. (2019). Spectral analysis of the September 2017 solar energetic particle events. *Space Weather*, *17*(3), 419–437. https://doi.org/10.1029/2018sw002085

Cane, H., Reames, D., & Von Rosenvinge, T. (1991). Solar particle abundances at energies of greater than 1 MeV per nucleon and the role of interplanetary shocks. *The Astrophysical Journal*, *373*, 675–682. https://doi.org/10.1086/170088

Chen, Y., Friedel, R., Reeves, G., Onsager, T., & Thomsen, M. (2005). Multisatellite determination of the relativistic electron phase space density at geosynchronous orbit: Methodology and results during geomagnetically quiet times. *Journal of Geophysical Research*, *110*(A10). https://doi.org/10.1029/2004ja010895

Dungey, J., Hess, W., & Nakada, M. (1965). Theoretical studies of protons in the outer radiation belt. In *Space research conference* (p. 399).

Evans, D., & Greer, M. (2000). *Polar-orbiting environmental satellite space environment monitor. 2000.*

GOES, N. (2010). *Series Data Book, revision d (Tech. Rep.).* CDRL PM-1-1-03. February 2005, Boeing Corp.

Gold, R., Krimigis, S., Hawkins, S., Haggerty, D., Lohr, D., Fiore, E., et al. (1998). Electron, proton, and alpha monitor on the advanced composition explorer spacecraft. *The Advanced Composition Explorer Mission*, 541–562. https://doi.org/10.1007/978-94-011-4762-0_19

Gopalswamy, N., Yashiro, S., Mäkelä, P., Xie, H., Akiyama, S., & Monstein, C. (2018). Extreme kinematics of the September 10, 2017 solar eruption and the spectral characteristics of the associated energetic particles. *The Astrophysical Journal Letters*, *863*(2), L39. https://doi.org/10.3847/2041-8213/aad86c

Gopalswamy, N., Yashiro, S., Thakur, N., Mäkelä, P., Xie, H., & Akiyama, S. (2016). The July 23, 2012 backside eruption: An extreme energetic particle event? *The Astrophysical Journal*, *833*(2), 216. https://doi.org/10.3847/1538-4357/833/2/216

Green, J. (2013). *MEPED telescope data processing theoretical basis document version 1.0 (Tech. Rep.).* Boulder, Colo: NOAA Technical Memorandum, Space Environ. Lab.

Iyemori, T., & Rao, D. (1996). *Decay of the Dst field of geomagnetic disturbance after substorm onset and its implication to storm-substorm relation.*

Kirby, K., Artis, D., Bushman, S., Butler, M., Conde, R., Cooper, S., et al. (2012). Radiation belt storm probes—observatory and environments. *Space Science Reviews*, *179*(1–4), 59–125. https://doi.org/10.1007/s11214-012-9949-2

Koons, H., & Fennell, J. (2006). Space weather effects on communications satellites. *URSI Radio Science Bulletin*, *2006*(316), 27–41.

Le, G., Cai, Z., Wang, H., & Zhu, Y. (2012). Solar cycle distribution of great geomagnetic storms. *Astrophysics and Space Science*, *339*(1), 151–156. https://doi.org/10.1007/s10509-011-0960-y

Le, G., & Han, Y. (2005). Analysis of the acceleration process of seps by an interplanetary shock for Bastille Day event. In K. Dere, J. Wang, & Y. Yan (Eds.), *Coronal and stellar mass ejections* (Vol. 226, pp. 346–349). https://doi.org/10.1017/S1743921305000840

Li, C., Dai, Y., Vial, J.-C., Owen, C., Matthews, S., Tang, Y., et al. (2009). Solar source of energetic particles in interplanetary space during the December 13, 2006 event. *Astronomy & Astrophysics*, *503*(3), 1013–1021. https://doi.org/10.1051/0004-6361/200911986

Machol, J. (2012). *POES/METOP SEM-2 omni flux algorithm theory and software description.* version 1.0 (p. 43). NOAA National Geophysical Data Center.

Mauk, B., Fox, N. J., Kanekal, S., Kessel, R., Sibeck, D., & Ukhorskiy, A. (2012). Science objectives and rationale for the radiation belt storm probes mission. In *The van Allen probes mission* (pp. 3–27). Springer. https://doi.org/10.1007/978-1-4899-7433-4_2

Mewaldt, R., Cohen, C., Labrador, A., Leske, R., Mason, G., Desai, M., et al. (2005). Proton, helium, and electron spectra during the large solar particle events of October–November 2003. *Journal of Geophysical Research*, *110*(A9). https://doi.org/10.1029/2005ja011038

Miller, J. (1997). Electron acceleration in solar flares by fast mode waves: Quasi-linear theory and pitch-angle scattering. *The Astrophysical Journal*, *491*(2), 939–951. https://doi.org/10.1086/305004

Moldwin, M. (2008). *An introduction to space weather* (Vol. 10). Cambridge: Cambridge University Press.

O'Brien, T. P., Mazur, J. E., & Looper, M. D. (2018). Solar energetic proton access to the magnetosphere during the September 10–14, 2017 particle event. *Space Weather*, *16*(12), 2022–2037.

Qin, G., & Shalchi, A. (2009). Pitch-angle diffusion coefficients of charged particles from computer simulations. *The Astrophysical Journal*, *707*(1), 61–66. https://doi.org/10.1088/0004-637x/707/1/61

Redmon, R., Rodriguez, J., Green, J., Ober, D., Wilson, G., Knipp, D., et al. (2015). Improved polar and geosynchronous satellite data sets available in common data format at the coordinated data analysis web. *Space Weather*, *13*(5), 254–256. https://doi.org/10.1002/2015sw001176

Rodriguez, J., Krosschell, J., & Green, J. (2014). Intercalibration of GOES 8-15 solar proton detectors. *Space Weather*, *12*(1), 92–109. https://doi.org/10.1002/2013sw000996

Sharykin, I. N., & Kosovichev, A. G. (2018). Onset of photospheric impacts and helioseismic waves in X9. 3 solar flare of September 6, 2017. *The Astrophysical Journal*, *864*(1), 86. https://doi.org/10.3847/1538-4357/aad558

Snyder, J. (1967). Radiation hazard to man from solar proton events. *Journal of Spacecraft and Rockets*, *4*(6), 826–828. https://doi.org/10.2514/3.28971

Stratton, J., Harvey, R., & Heyler, G. (2012). Mission overview for the radiation belt storm probes mission. In *The van Allen probes mission* (pp. 29–57). Springer. https://doi.org/10.1007/978-1-4899-7433-4_3

Sun, X., & Norton, A. A. (2017). *Super-flaring active region 12673 has one of the fastest magnetic flux emergence ever observed. arXiv preprint arXiv:1711.08383.*

Turner, D., & Li, X. (2008). Radial gradients of phase space density of the outer radiation belt electrons prior to sudden solar wind pressure enhancements. *Geophysical Research Letters*, *35*(18). https://doi.org/10.1029/2008gl034866

Von Rosenvinge, T., Barbier, L., Karsch, J., Liberman, R., Madden, M., Nolan, T., et al. (1995). The energetic particles: Acceleration, composition, and transport (EPACT) investigation on the wind spacecraft. *Space Science Reviews*, *71*(1–4), 155–206. https://doi.org/10.1007/bf00751329

Wang, J., Shi, Z., Wang, H., & Lue, Y. (1996). Flares and the magnetic nonpotentiality. *The Astrophysical Journal*, *456*, 861. https://doi.org/10.1086/176703

Warren, H. P., Brooks, D. H., Ugarte-Urra, I., Reep, J. W., Crump, N. A., & Doschek, G. A. (2018). Spectroscopic observations of current sheet formation and evolution. *The Astrophysical Journal*, *854*(2), 122. https://doi.org/10.3847/1538-4357/aaa9b8

Yan, Y., Pick, M., Wang, M., Krucker, S., & Vourlidas, A. (2006). A radio burst and its associated CME on March 17, 2002. *Solar Physics*, *239*(1), 277–292. https://doi.org/10.1007/s11207-006-0202-6

Zhang, J., Dere, K., Howard, R., Kundu, M., & White, S. (2001). On the temporal relationship between coronal mass ejections and flares. *The Astrophysical Journal*, *559*(1), 452–462. https://doi.org/10.1086/322405

Zwickl, R., Doggett, K., Sahm, S., Barrett, W., Grubb, R., Detman, T., et al. (1998). The NOAA real-time solar-wind (RTSW) system using ace data. In *The advanced composition explorer mission* (pp. 633–648). Springer. https://doi.org/10.1007/978-94-011-4762-0_22